Title
Defect reduction in (11(2)over-bar0) a-plane gallium nitride via lateral epitaxial overgrowth by hydride vapor-phase epitaxy

Permalink
https://escholarship.org/uc/item/3mb4z0x9

Journal
Applied Physics Letters, 83(4)

ISSN
0003-6951

Authors
Haskell, B A
Wu, F
Craven, M D
et al.

Publication Date
2003-07-01

Peer reviewed

APPLIED PHYSICS LETTERS VOLUME 83, NUMBER 4 28 JULY 2003

Defect reduction in $(11\bar{2}0)$ *a*-plane gallium nitride via lateral epitaxial overgrowth by hydride vapor-phase epitaxy

B. A. Haskell,[a),b)] F. Wu,[a)] M. D. Craven,[a)] S. Matsuda, P. T. Fini,[a)] T. Fujii,[a)] K. Fujito,[a)]
S. P. DenBaars,[a)] J. S. Speck,[a)] and Shuji Nakamura[a)]
Materials Department, University of California, Santa Barbara, California 93106-5050

(Received 25 March 2003; accepted 21 May 2003)

This letter reports on the reduction in extended-defect densities in *a*-plane $(11\bar{2}0)$ GaN films achieved via lateral epitaxial overgrowth (LEO) by hydride vapor phase-epitaxy. A variety of dielectric mask patterns was used to produce 8–125-μm-thick, fully coalesced nonpolar GaN films. The nanometer-scale pit densities in the overgrown regions were less than $3\times10^6\ \mathrm{cm}^{-2}$ compared to $\sim10^{10}\ \mathrm{cm}^{-2}$ in the direct-growth *a*-plane GaN. Cathodoluminescence revealed a fourfold increase in luminous intensity in the overgrown material compared to the window material. X-ray rocking curves indicate the films were free of wing tilt within the sensitivity of the measurements. Whereas non-LEO *a*-plane GaN exhibits basal plane stacking fault and threading dislocation densities of $10^5\ \mathrm{cm}^{-1}$ and $10^9\ \mathrm{cm}^{-2}$, respectively, the overgrown LEO material was essentially free of extended defects. The basal plane stacking fault and threading dislocation densities in the wing regions were below the detection limits of $\sim5\times10^6\ \mathrm{cm}^{-2}$ and $3\times10^3\ \mathrm{cm}^{-1}$, respectively. © *2003 American Institute of Physics.* [DOI: 10.1063/1.1593817]

Gallium nitride and its alloys with indium and aluminum nitride have attracted significant attention in recent years due to their successful incorporation in visible and ultraviolet light-emitting diodes[1] (LEDs), blue/violet laser diodes,[2] and high-power electronic devices.[3] The vast majority of these devices are grown parallel to the [0001] *c*-axis of the wurtzite GaN crystal structure. While *c*-plane-oriented (Al,In,Ga)N films are the most commonly grown nitrides for device applications, *c*-axis-oriented optoelectronic devices in particular suffer from undesirable spontaneous and piezoelectric polarization effects. GaN-based quantum structures grown along nonpolar directions, such as $[10\bar{1}0]$[4] and $[11\bar{2}0]$[5,6] have been demonstrated to be free of these polarization effects.

As bulk GaN crystals or appreciable size are not available, hydride vapor-phase epitaxy (HVPE) has been used to heteroepitaxially grow thick (10–300+μm) *c*-plane GaN films to serve as homoepitaxial substrates for subsequent device growth by molecular-beam epitaxy and metalorganic chemical vapor deposition (MOCVD).[7,8] Recently, we have reported on the growth of planar $(11\bar{2}0)$ *a*-plane GaN by HVPE,[9] demonstrating the potential for fabrication of nonpolar GaN substrates. The films described in that letter exhibited threading dislocation densities on the order of $10^9\ \mathrm{cm}^{-2}$, in addition to a high ($10^5\ \mathrm{cm}^{-1}$) density of intrinsic basal plane stacking faults attributed to stacking errors on the nitrogen face $(000\bar{1})$ in the early stages of growth.[10] However, ideal GaN substrates would be essentially free of threading dislocations, stacking faults, and macroscopic defects that could affect the quality of the device layers subsequently regrown upon them.

Lateral epitaxial overgrowth (LEO) has been demonstrated to be an effective approach for the reduction of extended defect densities in *c*-plane GaN by both MOCVD[11–14] and HVPE.[15–18] LEO performed by MOCVD has yielded similar defect reduction in *a*-plane GaN films.[19] The present work reports on the elimination of extended defects and morphological improvements recently demonstrated in HVPE-grown *a*-plane GaN films via LEO.

The masks for the LEO process were prepared by utilizing conventional photolithographic processing and wet etching to ~1300-Å-thick plasma-enhanced chemical-vapor-deposited SiO_2 dielectric layers. A variety of mask designs was investigated, including arrays of circular apertures, parallel stripes oriented along the [0001] direction, parallel stripes oriented along the $[1\bar{1}00]$ direction, and nonparallel stripes in a ‘‘wagon-wheel’’ pattern. The LEO growth process was carried out in a conventional three-zone horizontal directed-flow HVPE system.[9] Typical vertical growth rates ranged from 16 to 50 μm/h at a substrate temperature of ~1040 °C. A variety of mask geometries yielded coalesced films; in particular, the use of masks consisting of periodic arrays of $[1\bar{1}00]$-oriented stripes allowed full 50-mm-diameter *a*-plane GaN wafers to be coalesced.

Figure 1(a) gives a schematic representation of the $[1\bar{1}00]$ stripe geometry that was used for the samples to be discussed subsequently. Interrupted growths have shown that the (0001) Ga-face wing advances roughly six times as rapidly as the $(000\bar{1})$ N-face wing. This ratio indicates that the relative growth rate of the $(000\bar{1})$ wing is measurably greater in HVPE growth compared to MOCVD growth of GaN, in which the ratio of Ga- to N-face growth is ~10.[19] One benefit of the large difference in lateral growth rates between the {0001} faces is that the coalescence front was offset towards the N-face side of the window region, yielding a broad wing region uninterrupted by defective coalescence fronts. Figure

---

[a)] NICP/ERATO JST, UCSB Group, University of California, Santa Barbara, CA 93106-5050

[b)] Electronic mail: bhaskell@engineering.ucsb.edu

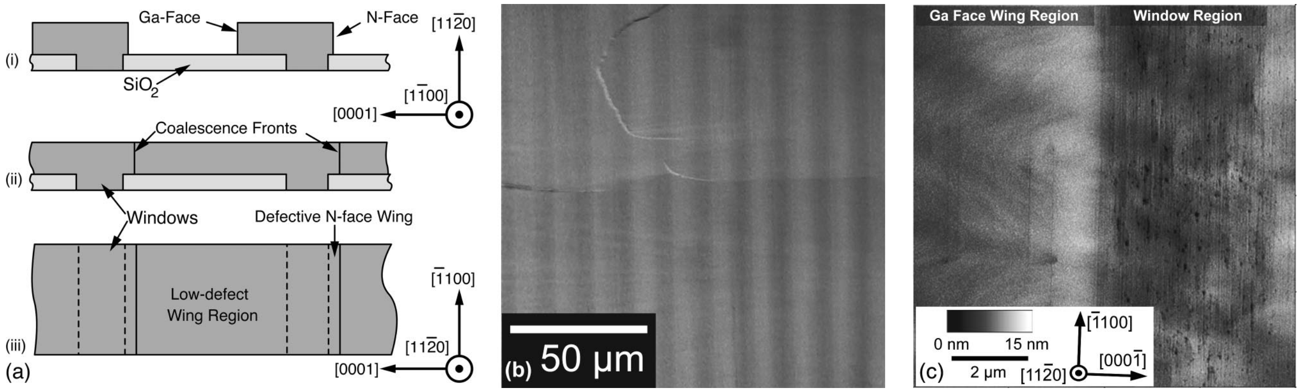

FIG. 1. (a) Schematics of LEO growth using mask bars oriented along the GaN $[1\bar{1}00]$ direction. (i) Cross section of uncoalesced stripes. (ii) Cross section of coalesced stripes showing the offset coalescence front. (iii) Plan view of coalesced stripes identifying the large low-defect wing region. (b) Nomarski optical contrast micrograph of a coalesced LEO a-plane GaN film. (c) 10-μm AFM image of coalesced $[1\bar{1}00]$-oriented GaN stripes.

1(b) shows a Nomarski optical contrast micrograph of a 20-μm-thick coalesced LEO film formed with $[1\bar{1}00]$-oriented stripes. The faint ‘‘fish scale’’-like feature on the upper portion of the image demonstrated that the film's surface is in focus, while the refractive index contrast from the SiO_2 allowed the out-of-focus mask pattern to be observed.

Atomic force microscopy (AFM) was performed to compare the surface quality in the window and wing regions of the a-plane LEO films. Figure 1(c) shows a 10×10-μm AFM topograph of two coalesced stripes. The window region appeared as the darker band of pitted material, with the coalescence front roughly 1 μm to the left of the window. The Ga-face wing, apparent on the left side of the image, had superior surface quality, exhibiting average pit densities of less than 3×10^6 cm^{-2}, compared to $\sim10^9$ cm in the window regions. The rms roughness of the wing regions was less than 0.9 nm (11.9-nm peak-to-valley height), compared to 1.3 nm (20.8-nm peak-to-valley) in the window regions.

Figures 2(a) and 2(b) are cross-sectional scanning electron microscopy (SEM) images of LEO wafers patterned with a periodic array of $[1\bar{1}00]_{GaN}$-oriented SiO_2 stripes. The inclined cross-section in Fig. 2(a) demonstrates the sharply vertical {0001} sidewalls that are prevalent for $[1\bar{1}00]$-oriented stripes throughout lateral growth and immediately preceding coalescence. Figure 2(b) shows a cross-sectional view of four coalesced GaN stripes. Only contrast variation at the film–template interface due to charging effects allows the window and wing regions to be distinguished. Figure 2(c) is a plan-view SEM image of a coalesced film, again with a mask of SiO_2 stripes oriented along the GaN $[1\bar{1}00]$ direction. The surface was flat and almost featureless, except for a few faint irregular ridges. These ridges manifested themselves in the corresponding cathodoluminescence (CL) image in Fig. 2(d) as irregular dark features. Figure 2(d) is a CL image of the surface in Fig. 2(c) imaged at 365 nm, with lighter shades of gray indicating greater luminous intensity. The window regions in the CL image are apparent as the dark vertical bands. Because of the proximity of the coalescence front to the windows, large, relatively defect-free regions result from the use of $[1\bar{1}00]$ stripes, providing ample surface area for the fabrication of devices. The narrow, dark horizontal lines oriented along the $\langle 0001\rangle$ direction did not appear to correspond to surface features. The cause of this decreased luminescence is a point of ongoing investigation, although preliminary transmission electron microscopy (TEM) results indicate that clusters of stacking faults lying on the prismatic $\{1\bar{1}00\}$ planes may account for these dark lines.

The structural quality of the a-plane LEO films was characterized by x-ray diffraction and TEM. X-ray rocking curves of the $11\bar{2}0$ GaN reflection taken perpendicular to the LEO stripe direction were single-peaked, indicating a lack of measurable tilt in the coalesced films. Narrowing of both on- and off-axis reflections was observed in the LEO films compared to planar a-plane GaN films grown directly on r-plane

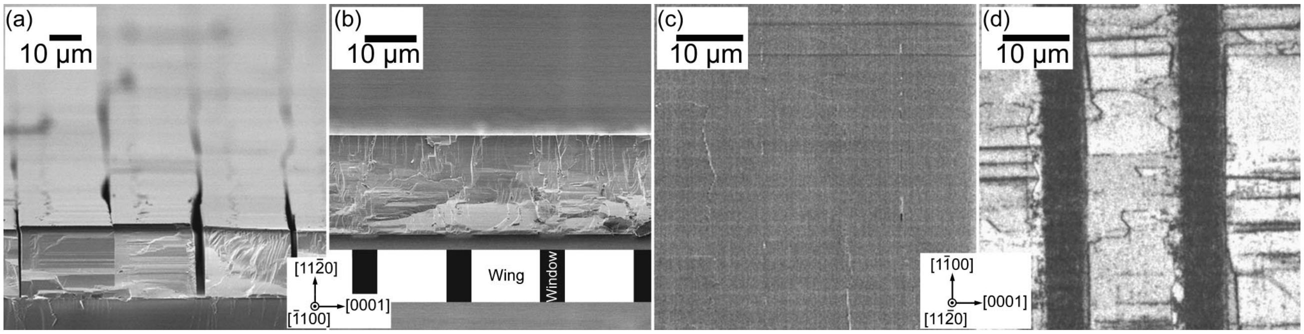

FIG. 2. (a) Cross-sectional SEM image of parallel LEO stripes approaching coalescence. (b) Cross-sectional SEM image showing coalesced stripes. The black bars below the LEO film show the locations of the windows. (c) Plan-view SEM image of the coalesced region pictured in (d), which is a monochromatic CL image of the region shown in (c) at 365 nm. The mask in each case consisted of parallel SiO_2 stripes along the GaN $[1\bar{1}00]$ direction.

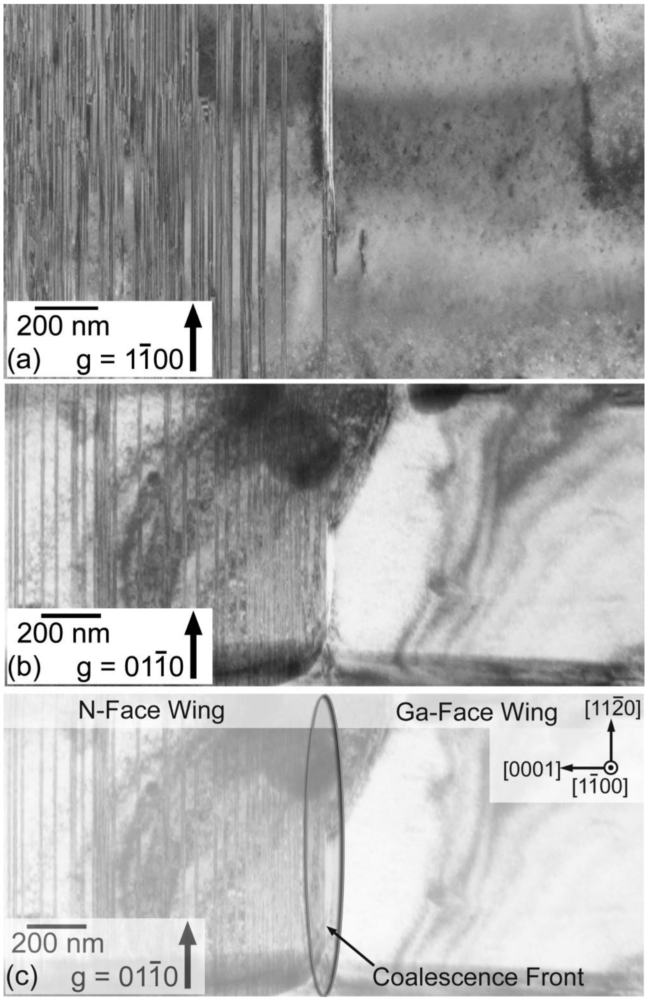

FIG. 3. (a) Plan-view TEM of coalesced [$1\bar{1}00$] stripes. (b) Corresponding cross-sectional TEM image with (c) explanation of salient features.

sapphire.[9] Typical full widths at half-maxima for the $11\bar{2}0$ and $10\bar{1}0$ reflections were 750 and 1250 arcsec, respectively.

Figure 3 shows plan-view and cross-sectional TEM images of a LEO film imaged with **g** vectors of $1\bar{1}00$ and $01\bar{1}0$, respectively. In agreement with observations from AFM and CL, the window regions exhibited high threading dislocation ($\sim 9\times 10^9$ cm^{-2}) and stacking fault ($\sim 4\times 10^5$ cm^{-1}) densities. In contrast, the Ga-face wing region was essentially free of both dislocations and stacking faults, with densities below the images' resolutions of $\sim 5\times 10^6$ cm^{-2} and $\sim 3\times 10^3$ cm^{-1}, respectively. The N-face wing region was also threading dislocation-free, though basal plane stacking faults and Shockley partial dislocations terminating the faults remained prevalent.

The results just described have demonstrated that substantial reduction in morphological and structural defects in a-plane GaN may be readily achieved by lateral epitaxial overgrowth with hydride vapor phase epitaxy. The reduction in threading dislocation density in the overgrown GaN is accompanied by a significant improvement in surface morphology and luminescence compared to non-LEO planar a-plane GaN. Coupling LEO with the comparably high growth rates achievable by HVPE bodes well for the fabrication of high-quality nonpolar gallium nitride substrates.

This work made use of the MRL Central Facilities supported by the National Science Foundation under Award No. DMR00-80034.

[1] T. Nishida and N. Kobayashi, Phys. Status Solidi A **188**, 113 (2001).
[2] S. Nakamura, G. Fasol, and S. J. Pearton, *The Blue Laser Diode* (Springer, New York, 2000).
[3] L. F. Eastman and U. K. Mishra, IEEE Spectrum **39**, 28 (2002).
[4] P. Waltereit, O. Brandt, A. Trampert, H. T. Grahn, J. Menniger, M. Ramsteiner, M. Reiche, and K. H. Ploog, Nature (London) **406**, 865 (2000).
[5] M. D. Craven, P. Waltereit, F. Wu, J. S. Speck, and S. P. DenBaars, Jpn. J. Appl. Phys. **42**, L235 (2003).
[6] H. M. Ng, Appl. Phys. Lett. **80**, 4369 (2002).
[7] K. Motoki, T. Okahisa, N. Matsumoto, M. Matsushima, H. Kimura, H. Kasai, K. Takemoto, K. Uematsu, T. Hirano, M. Nakayama, S. Nakahata, M. Ueno, D. Hara, Y. Kumagai, A. Koukitu, and H. Seki, Jpn. J. Appl. Phys., Part 2 **40**, L140 (2001).
[8] T. Paskova, P. P. Paskov, V. Darakchieva, S. Tungasmita, J. Birch, and B. Monemar, Phys. Status Solidi A **183**, 197 (2001).
[9] B. A. Haskell, F. Wu, M. D. Craven, S. Matsuda, P. T. Fini, S. P. DenBaars, J. S. Speck, and S. Nakamura (unpublished).
[10] F. Wu, M. D. Craven, S. H. Lim, and J. S. Speck, J. Appl. Phys. **94**, 942 (2003).
[11] T. S. Zheleva, N. Ok-Hyun, M. D. Bremser, and R. F. Davis, Appl. Phys. Lett. **71**, 2472 (1997).
[12] N. Ok-Hyun, M. D. Bremser, T. S. Zheleva, and R. F. Davis, Appl. Phys. Lett. **71**, 2638 (1997).
[13] H. Marchand, J. P. Ibbetson, P. T. Fini, P. Kozodoy, S. Keller, S. DenBaars, J. S. Speck, and U. K. Mishra, MRS Internet J. Nitride Semicond. Res. **3**, 3 (1998).
[14] H. Marchand, X. H. Wu, J. P. Ibbetson, P. T. Fini, P. Kozodoy, S. Keller, J. S. Speck, S. P. DenBaars, and U. K. Mishra, Appl. Phys. Lett. **73**, 747 (1998).
[15] A. Sakai, H. Sunakawa, A. Kimura, and A. Usui, Appl. Phys. Lett. **76**, 442 (2000).
[16] O. Parillaud, V. Wagner, H. Bühlmann, and M. Ilegems, MRS Internet J. Nitride Semicond. Res. **3**, 40 (1998).
[17] G. Nataf, B. Beaumont, A. Bouille, S. Haffouz, M. Vaille, and P. Gibart, J. Cryst. Growth **192**, 73 (1998).
[18] H. Tsuchiya, K. Sunaba, T. Suemasu, and F. Hasegawa, J. Cryst. Growth **189/190**, 395 (1998).
[19] M. D. Craven, S. H. Lim, F. Wu, J. S. Speck, and S. P. DenBaars, Appl. Phys. Lett. **81**, 1201 (2002).